

# (Semi) regular tetrahedral tilings

Alexej Kolcun

Institute of Geonics, Czech Academy of Sciences  
Studentská 1768  
708 00 Ostrava, Czech Republic  
alexej.kolcun@ugn.cas.cz

## ABSTRACT

Triangulation 2D and 3D methods represent an important part of numerical modeling process (e.g. FEM). In many applications it is suitable to use triangulations with a regular structure. Moreover, decomposition with a limited number of different types of tetrahedra enables to reduce the storage and computational demands in the whole modeling process. The submitted contribution presents an overview of possible 3D decompositions using one tetrahedron (regular tilings). These decompositions are confronted with decompositions using six different types of tetrahedra (orthogonal structured tilings). Considering the shape expressivity of particular methods, the paper presents a structure of possible decompositions and comparison of storage demands of the used decompositions.

## Keywords

tetrahedron, regular tessellation, voxel grid, conform decomposition.

## 1. INTRODUCTION

The tasks connected with space decomposition have been presented in various research areas for a long time, and they are connected with Hilbert's 18<sup>th</sup> problem [H], [G 1980]. The whole raster graphic concept can be seen from this point of view. A different raster concept, based on regular hexagonal mesh, is analyzed e.g. in [M 2005].

Within the numerical methods development, space discretization has become an important tool of shape expressivity. For example, in the finite element modeling (FEM), the domain of interest is decomposed to simple polyhedral elements. In the simplest case, the triangles for 2D tasks and tetrahedra for 3D tasks are used. Nowadays, there is a wide range of generators used for decomposition (meshes), e.g. [E 2001], [F 2000].

Surprisingly, we may expect that with HW development the role of regular meshes for physically based modeling will grow. For example, CT

technologies of 3D scanning give us information about geometry in a regular rectangular grid. Thus, the originally demanding preparation of the analyzed domain geometry is possible to fully automatize in a very simple way, [P 2003], [A 2007].

Advantages of this approach:

1. simplicity,
2. velocity,
3. relatively small storage demands (hereby described geometry contains a huge amount of grid vertices, but it is not necessary to keep their coordinates – these can be simply calculated),
4. regular structure of the equations system which must be solved.

The results of this approach significantly exceed its disadvantages:

1. From the numerical model viewpoint, the discretization error – aliasing – of boundaries of particular domain areas has only a very local character [A 2007].
2. Moreover, this error may be eliminated by the pixel/voxel partitioning; either from the geometry viewpoint – Fig. 1, [L 2013] or from the numerical solution viewpoint – Fig. 2. Even though this method is only partial, it is very effective in many cases.
3. Using Marching Cubes and Marching Tetrahedra methods (originally developed

Permission to make digital or hard copies of all or part of this work for personal or classroom use is granted without fee provided that copies are not made or distributed for profit or commercial advantage and that copies bear this notice and the full citation on the first page. To copy otherwise, or republish, to post on servers or to redistribute to lists, requires prior specific permission and/or a fee.

directly for these rectangular grids), it is possible to eliminate effectively this discretization error, e.g. [P 2005].

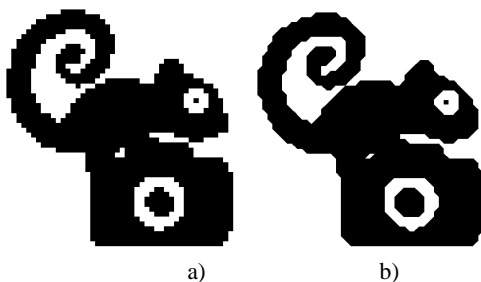


Figure 1 a) Raster representation and b) partitioned raster representation [L2013].

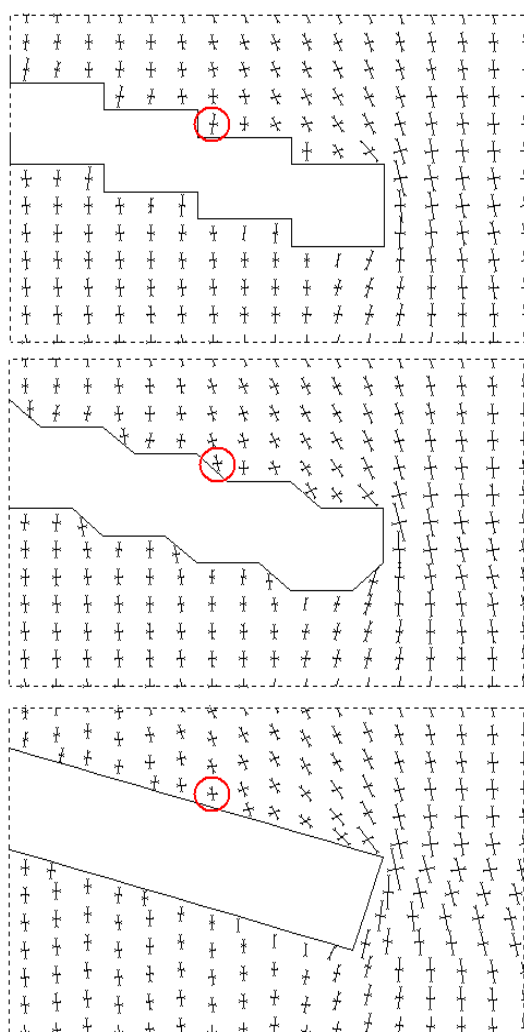


Figure 2 Local character of the influence of the domain boundary aliasing to the stress tensor.

Next approach of regular rasterization [L 2013] can be based on equilateral triangles – Fig. 3a): regular rectangular mesh (black lines) is deformed and proper diagonals (gray lines) are added. In this case, the major part of triangles (all except for the

boundary ones) is equilateral. Fig. 3b) gives the example of such rasterization. While in the concept of the partitioning from Fig. 1b) the choice of the diagonals depends on material (color) distribution in the raster grid, the partitioning in the concept from Fig. 3a) is regular – ‘zig-zag’.

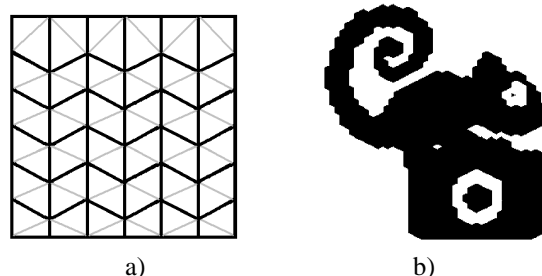


Figure 3 a) Generalized rasterization based on a ‘deformed’ regular grid (black lines), supplemented with diagonals (gray lines), b) example of rasterized image [L2013].

The paper presents an overview of all known space decomposition methods to identical tetrahedra (regular tetrahedral tiling). This mechanism influences the result of the Marching Cubes (Tetrahedra) method.

While Sommerville decompositions (Section 2.1) are relatively well known and widely used in the computer modeling area, Goldberg decompositions (Section 2.2) are considerably less known among the computer graphic community. Mutual dependences of these decompositions are mentioned.

The method of orthogonal structured tilings (decomposition to several different tetrahedra) is also described.

A comparison of the shape expressivity of mentioned methods is presented.

## 2. REGULAR TETRAHEDRAL TILINGS

At present, two approaches of regular tetrahedral tilings are known [G 1978], [S 1981].

1. decompositions obtained by partitioning of a regular rectangular grid using only one type of tetrahedral element (Sommerville),
2. decompositions obtained by partitioning of a 3-sided prism (Goldberg).

### 2.1 Regular rectangular grid partitioning

Let us consider a regular rectangular grid (voxel grid). Its basic volume element is an orthogonal prism (brick). There are five partitioning tetrahedra obtained by its decomposition. The basic one is tetrahedron I. (Fig. 4), where vertex D is the centre of the cube, C is the centre of the right side.

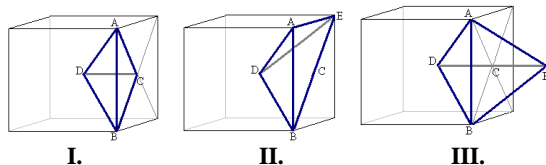


Figure 4 Tiling tetrahedra, part 1.

The tetrahedron II (Fig. 4) is a union of two tetrahedra of the type I with common face ACD. The tetrahedron III is a union of the two tetrahedra of the type I with common face ABC. Table 1 shows the mutual rate of edges of the described tetrahedra.

<b>I.</b> ABDC	AB 2	BD $\sqrt{3}$	AD $\sqrt{3}$	AC $\sqrt{2}$	BC $\sqrt{2}$	DC 1
<b>II.</b> ABDE	AB 2	BD $\sqrt{3}$	AD $\sqrt{3}$	AE 2	BE $2\sqrt{2}$	DE $\sqrt{3}$
<b>III.</b> ABDF	AB 2	BD $\sqrt{3}$	AD $\sqrt{3}$	AF $\sqrt{3}$	BF $\sqrt{3}$	DF 2
<b>IV.</b> ABDH	AB 2	BD $\sqrt{3}$	AD $\sqrt{3}$	AH $\sqrt{5}/2$	BH $\sqrt{5}/2$	DH $\sqrt{5}/2$
<b>V.</b> ABJF	AB 2	BJ $\sqrt{11}/2$	AJ $\sqrt{3}/2$	AF $\sqrt{3}$	BF $\sqrt{3}$	JF $\sqrt{11}/2$

Table 1 Lengths of edges of the tiling tetrahedra for a rectangular grid partitioning.

Note that the tetrahedron II is asymmetrical and in this case, the decomposition has to contain mutually symmetric pairs of tetrahedra. We say that such a regular tiling is asymmetrical.

Next two types of partitioning tetrahedra are derived from the type III:

Let us consider the node G – the centre of the edge AB and the node C – the centre of the edge DF (Fig. 4 III'). We abbreviate H – the centre of the segment CG. It is obvious that H is the centre of the sphere circumscribed to the tetrahedron ABDF. Because of the fact that the faces of ABDF – III (Fig. 4, Tab. 1) are identical, using the vertex H we can decompose this tetrahedron to four identical tetrahedra ABDH, BAFH, DFAH, and FDBH. Thus the ABDH tetrahedron generates a symmetrical tiling (Fig. 5 IV.).

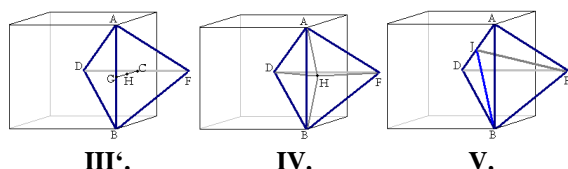


Figure 5 Tiling tetrahedra, part 2.

Let J be the centre of the edge AD. Then the tetrahedra ABFJ and DFBJ are symmetrical, i.e.

tetrahedron ABFJ generates an asymmetrical tiling (Fig. 5 V.).

### 2.2 Decompositions from 3-sided prism

Let us consider a right prism whose normal section is an equilateral triangle of edge  $e$ . On the edges of the prism we generate vertices by „gradual rolling up“ (red polyline) with given shift  $h$  (Fig. 6).

The tetrahedron ABCD – VI. obviously generates a tiling: let us consider neighbor tetrahedra ABCD and BCDB'. Each of them contains three edges of length  $a$  – red, (AB,BC,CD, BC,CD,DB' respectively), two edges of length  $b$  – blue, (AC,BD, BD,CB' respectively), one edge of length  $3h$  – black AD, BB' respectively). Moreover, both tetrahedra ABCD and BCDB' have the same orientation.

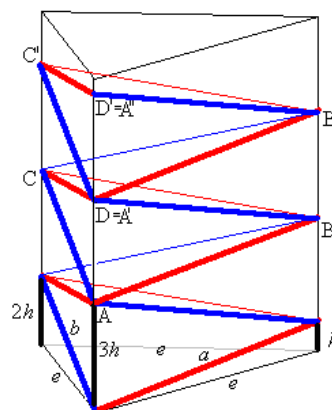


Figure 6 Basic partition of 3-sided prism – VI.

Since the ratio  $h/e$  is arbitrary, there is a continuous infinity of tiling tetrahedra of this type where

$$a = \sqrt{e^2 + h^2}, \tag{1}$$

$$b = \sqrt{e^2 + 4h^2}. \tag{2}$$

Another two tiling tetrahedra – VII., VIII., (Fig. 7) can be derived in the following way:

vertex E is the centre of the edge AD, and so the triangle BCE is isosceles, i.e. BE=CE=c, where

$$c = \sqrt{e^2 + \left(\frac{h}{2}\right)^2} = \frac{\sqrt{4e^2 + h^2}}{2}. \tag{3}$$

Similarly the vertex F is the centre of the edge BC and so the triangle ADF is isosceles, i.e. AF=DF=d. Moreover, angle  $\angle BFD$  is right one, so

$$d = \sqrt{b^2 - \left(\frac{a}{2}\right)^2} = \sqrt{e^2 + 4h^2 - \frac{e^2 + h^2}{4}} = \frac{\sqrt{3e^2 + 15h^2}}{2}. \tag{4}$$

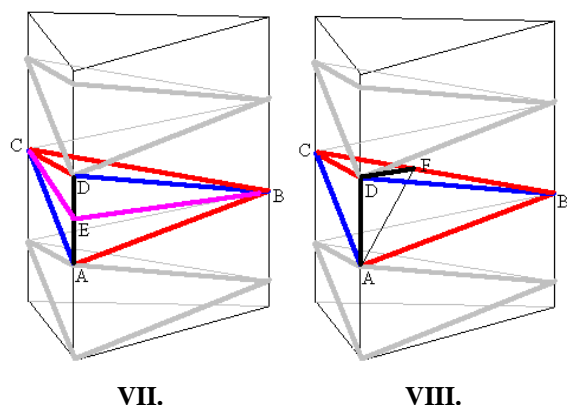


Figure 7 Tiling tetrahedra for 3-sided prism.

Table 2 shows the lengths of edges of partitioning tetrahedra for a 3-sided prism.

<b>VI.</b> <b>ABCD</b>	AB <i>a</i>	BC <i>a</i>	AC <i>b</i>	AD <i>3h</i>	BD <i>b</i>	CD <i>a</i>
<b>VII.</b> <b>ABCE</b>	AB <i>a</i>	BC <i>a</i>	AC <i>b</i>	AE <i>1,5h</i>	BE <i>c</i>	CE <i>c</i>
<b>VIII.</b> <b>ABFD</b>	AB <i>a</i>	BF <i>a</i>	AF <i>d</i>	AD <i>3h</i>	BD <i>b</i>	FD <i>d</i>

Table 2 Lengths of edges of the tiling tetrahedra for a 3-sided prism partitioning.

**Lemma 1.** The below described relations between tiling tetrahedra are valid:

- a) tetrahedron III. is a special case of the trahedron VI.,
- b) tetrahedron II. is a special case of the tetrahedron VII.,
- c) tetrahedron V. is a special case of the tetrahedron VII., VIII., respectively.

Proof: We shall prove relation a).

Let us consider tetrahedron VI. with

$$8h^2 = e^2.$$

According to (1), (2)

$$a = 3h, b = 2\sqrt{3}h, .$$

So, we have obtained tetrahedron III. – Tab. 1.

The rest of relations can be proved in similar way. More detailed proof in [G 1978]. *q.e.d.*

So far, there are not known any other regular tilings; on the other hand, their absence has not been proved yet [G 1978].

### 2.3 Decomposition conformity

Within the context of numerical modeling, the possibility of continuous interpolation is usually required. This is the reason why we suppose *conformity* of the used decomposition, i.e. the neighbor elements share either just one vertex, or the whole edge, or the whole face. This fact is automatically guaranteed by the above-described tilings, for the cases I. – V. excluding the decompositions based on tetrahedra II. For conformity of the tilings based on tetrahedron II, it is required that the neighbor voxels must be partitioned by the same diagonal (which is quite a natural assumption).

In the case of tetrahedra VI. – VIII., the „gradual rolling up“ in the neighbor 3-sided prism must be realized in the way of the mirror symmetry. Generally, if the tetrahedron VI. is asymmetric, the corresponding tilings are asymmetric too.

### 3. ORTHOHONAL STRUCTURED TILINGS

Let us show another way of decomposition. If we extenuate the condition of the tiling, i.e. we consider more than one type of tetrahedra (but the finite number), it is required that the tetrahedra vertices be the vertices created just from the original vertices from the orthogonal grid (*inscribed tetrahedra*). This decomposition is called *orthogonal structured one*.

The following relations are valid (the class of elements, decompositions respectively, is the set of elements, decompositions respectively, which differ only by the angle of rotation).

**Lemma 2.** There are 5 tetrahedra classes creating an orthogonal structured tiling (Fig. 8).

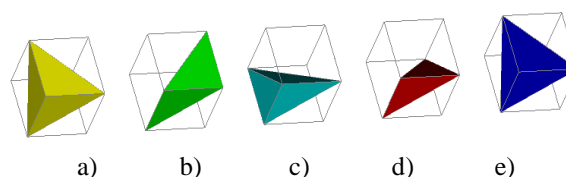


Figure 8 Tetrahedra of an orthogonal structured tiling.

The proof is simple; we obtain it by a detailed analysis of all four-element subsets of the orthogonal brick. *q.e.d.*

**Corollary:** there are 58 different tetrahedra inscribed into the cube.

**Lemma 3.** There is one class of the conform decomposition to 5 tetrahedra and 5 classes if the

conform decompositions to 6 tetrahedra (Fig. 8 – 9). [A 2003], [K 1999].

The proof results from the following facts.

1. The analysis of the conformal 5-element decompositions is trivial.
2. Conformal decomposition to 6-tetrahedra contains exactly one body diagonal.
3. The decomposition classes are uniquely determined by replacing the pair of tetrahedra b)c) from Fig. 8 with the pair a)d) – see Fig. 9a)-b). Similarly, we can replace other two pairs of tetrahedra b)c). The last type of decomposition is from Fig. 9e).

*q.e.d.*

Figures 9a) and e) show the most important decompositions often used within FEM modeling. Their important feature is that in both cases all three pairs of diagonals on opposite faces are mutually parallel.

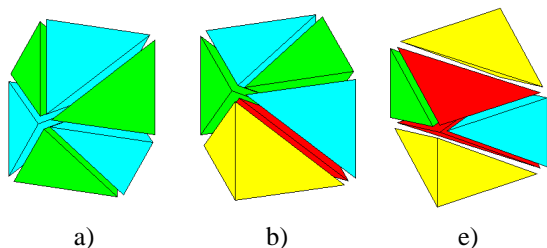


Figure 9 Examples of orthogonal structured tilings.

Figure 10 shows dual representation of all possible classes of conformal orthogonal structured tilings: tetrahedron is represented as a node, nodes are connected with the edge iff the tetrahedra are neighbor. The colors of tetrahedra from Figure 8 and nodes from Figure 10 mutually correspond. The abbreviation of tetrahedra from Fig. 9 and dual representations from Fig. 10 mutually correspond, i.e. the decomposition in Fig.9e corresponds to the representation in Fig. 10e).

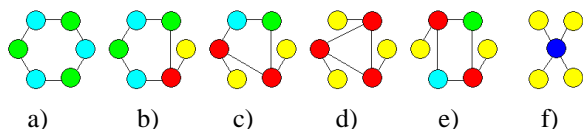


Figure 10 Dual representation of conform decompositions.

**Lemma 4.** There are 72 decompositions to 6 tetrahedra and two decompositions to 5 tetrahedra [K 1999].

The proof results from the analysis of rotating symmetries of particular classes.

Polyhedra from Fig 11 represent examples of well known Schönhardt’s polyhedra, for which there exists no conformal decomposition (e.g. [R 2005]).

The diagonal configurations from Fig. 11 may be characterized as follows: each vertex is incident to the limit of two diagonals and

- a) exactly two pairs of diagonals on the opposite sides are skew,
- b) all three pairs of diagonals on the opposite sides are skew.

Lemma 5 and 6 give finer results than [R 2005].

**Lemma 5.** For configuration of the surface diagonals from Figure 11a) there are nonconform decompositions only.

**Lemma 6.** For configuration of the surface diagonals from Figure 11b) there are no decompositions.

The proof of Lemmas 5 and 6 [K 1999] results from the fact, that the nonconform decomposition contains exactly two body diagonals.

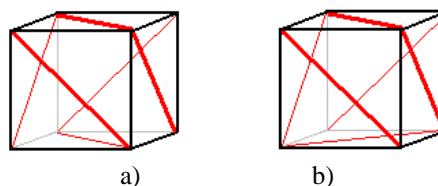


Figure 11 The surface diagonals configuration in which a) there are the nonconform decompositions only b) there is no decomposition.

Importance of last two Lemmas consists in conform decomposition algorithm:

1. Rectangular regular grid is generated.
2. Facial and space diagonals due to prescribed geometry are added.
3. Rest of diagonals is added – avoiding the configurations from the Fig. 11.

So far, there are not known any better algorithms for conform decompositions generation for general prescribed geometry.

Nonconformity decomposition can be solved effectively when the orthogonality of the initial grid is weakened [K 2002].

#### 4. SHAPE EXPRESSIVITY OF THE DECOMPOSITIONS

Let us consider a regular orthogonal grid with  $n$  vertices in each direction.

Table 3 shows the dependences of the number of vertices and the tetrahedra.

	Number of vertices	Number of tetrahedra
<b>I.</b>	$n^3 + (4n - 1)(n - 1)^2$	$24(n - 1)^3$

<b>II.</b>	$n^3 + (n-1)^3$	$12(n-1)^3$
<b>III.</b>	$n^3 + (n-1)^3$	$12(n-1)^3$
<b>IV.</b>	$n^3 + 13(n-1)^3$	$48(n-1)^3$
<b>V.</b>	$n^3 + 9(n-1)^3$	$24(n-1)^3$

Table 3: The vertices and tetrahedra in the decomposed voxel grid with  $n^3$  vertices.

On the other hand, all the structured decompositions to 6-tetrahedra keep their original number of vertices  $n^3$ . The number of elements is  $6(n-1)^3$ .

When editing the primary voxel grid, it is necessary not to be limited by the selection of the surface diagonals on the bricks. Obviously, each of the mentioned decompositions I. – V. allows to select the diagonals on the common face of bricks independently. To be more exact, all the decompositions, except for II, contain both diagonals on each side. In the case of the decomposition II, it is possible to select the face diagonals independently. Here the decomposition is directly determined by the surface diagonals selection.

From this point of view, it is meaningful to compare the orthogonal structured tiling (from Section 3) with the decomposition II only. Table 4 shows an overview of the results.

Decomposition	Number of vertices	Number of tetrahedra	Number of decompositions	The surface diagonals limits
<b>II.</b>	$\approx 2N$	$\approx 12N$	64	No
Struct.	$N$	$\approx 6N$	72	Yes

Table 4: Global characteristics of the orthogonal structured tilings and tiling II.

## 5. CONCLUSIONS

The submitted paper describes various approaches to generation of tetrahedral decompositions with a fixedly determined structure. Apart from the commonly used Sommerville decompositions based on a regular orthogonal grid, there are also analyzed Goldberg decompositions, which enable to use a more general discretization grid. Moreover, for the initial orthogonal grid there is also analyzed a more general decomposition to six tetrahedra, using a pentad of different tetrahedra. The basic properties of these decompositions are formulated and it is shown (Tab. 4) how extenuating the conditions may increase the possibilities of expression of various shapes.

## ACKNOWLEDGEMENTS

This work was supported by the projects

- RVO: 68145535,
- University of Ostrava, SP13/PRF/2013

## REFERENCES

- [A 2003] Apel, T., Duvelmeyer, N.: Transformation of Hexahedral FE-Mesh into Tetrahedral Meshes according to Quality Criteria, *Computing* 71 (2003), pp 293-304.
- [A 2007] Arbenz, P., Flaig, C.: On Smoothing in Voxel Based Finite Element Analysis of Trabecular Bone. In: LSSC2007 proc. (Lirkov, I., Margenov, S., Wasniewski J. eds.), *Lecture Notes in Computer Science* 4818, Springer 2008, pp. 69-77.
- [E 2001] Edelsbrunner, H.: *Geometry and Topology for Mesh Generation*, Cambridge University Press 2001.
- [F 2000] Frey, P.J., George, P.L.: *Mesh generation: Application to Finite Elements*, Hermes Science 2000.
- [G 1978] Goldberg M.: *Three Infinite Families of Tetrahedral Space/Fillers*, *Journal of Combinatorial Theory (A)* 16, 1978, pp.348-354.
- [G 1980] Grunbaum, B., Shepard, G.C.: Tilings with Congruent Tiles. *Bulletin of American Math. Soc.* Vol. 3, No.3, November 1980. pp. 951-973.
- [H] Hilbert's problems, [http://en.wikipedia.org/wiki/Hilbert%27s\\_problems](http://en.wikipedia.org/wiki/Hilbert%27s_problems)
- [K 1999] Kolcun, A.: The Quality of Meshes and FEM Computations, In WSCG proc. 1999 (V. Skala ed.), pp. 100-105.
- [K 2002] Kolcun, A.: Non-Conformity Problem in 3D Grid Decomposition, *Journal of WSCG*, Vol 10, No.1,(2002), pp. 249-254.
- [L 2013] Lubojacký, J.: *Basic algorithms of rasterization for generalized raster lattice* (in czech), Diploma Thesis, University of Ostrava, 2013.
- [M 2005] Middleton, M., Sivaswamy, J.: *Hexagonal Image processing*. Springer 2005.
- [P 2003] Práger, M.: *On a Construction of Fast Direct Solvers*, *Applications of Mathematics*, Vol. 48, No 3, 2003, pp. 225-236.
- [P 2005] Patera, J., Skala, V.: Centered Cubic Lattice Method Comparison. In. *Proc of Algorithm conf.* 2005, pp. 1-10.
- [R 2005] Rambau, J.: On a Generalization of Schonhardt's Polyhedron, *Combinatorial and Computational Geometry*, Vol. 52(2005), pp. 501-516.
- [S 1981] Senechal, M.: *Which tetrahedra Fill Space?*, *Mathematical Magazine*, Vol. 54, No. 5, 1981, pp. 227-243.